# Optical Mode Converter Integration With InP–InGaAsP Active and Passive Waveguides Using a Single Regrowth Process

Xuejin Yan, M. L. Mašanović, *Student Member, IEEE*, E. J. Skogen, *Student Member, IEEE*, Z. Hu, D. J. Blumenthal, *Senior Member, IEEE*, and L. A. Coldren, *Fellow, IEEE*

***Abstract*—A new method for integration of optical mode converters with InP-based photonic integrated circuits is described and demonstrated. The mode converter is integrated to a Sampled Grating DBR (SG-DBR) laser to demonstrate integration and to facilitate accurate fiber-coupling loss measurements. The entire fabrication process requires a single MOCVD regrowth, making it compatible with low-cost integration with other photonic components. The mode converter utilizes a vertically tapered geometry and yields a record 86% coupling efficiency using a lensed, uncoated, single-mode fiber. Cleaved fiber to InP-based waveguide coupling loss sensitivity is measured to be better than 1 dB with $\pm$1.85-$\mu$m lateral fiber misalignment and $\pm$1.5-$\mu$m transversal fiber misalignment.**

***Index Terms*—InP waveguides, mode converter, photonic integrated circuits, spot size converter.**

## I. Introduction

MONOLITHICALLY integrated InGaAsP–InP planar photonic integrated circuits (PICs) are a critical step to low-cost implementation of lightwave functions for optical communications and networks. Advanced PICs combine passive and active waveguide and grating elements to realize devices like widely tunable lasers, lasers integrated with modulators, tunable wavelength converters, and routers and other complex circuits that are not possible to implement using passive waveguide technologies alone. A key issue with InP-based PIC circuits is the inherent high coupling loss typically associated with coupling optical signals between fibers and InP-based waveguides. This loss originates in large mode-size mismatch of a single-mode InP-based waveguide to a standard single mode fiber. Although the coupling efficiency can be improved by using special lensed fibers or microoptical elements, it will complicate the device packaging and increase device cost, especially for planar light circuits that utilize multiple tilted-angle input and output waveguides.

Low-loss coupling is critical for many applications, including obtaining high launch power from integrated laser/modulator transmitters and optical wavelength converters or semiconductor optical amplifiers where coupling loss adds directly to the component noise figure. In addition to low-loss coupling, it is also important to reduce the sensitivity of alignment between the fiber and InP-based waveguide in order to reduce the cost of packaging these devices and reduce coupling efficiency sensitivity to environmental variations.

Manuscript received March 1, 2002; revised May 14, 2002. This work was supported under the Defense Advance Research Agency NGI Award MDA972-99-1-0006.

The authors are with the Department of Electrical and Computer Engineering, University of California at Santa Barbara, Santa Barbara, CA 93106 USA (e-mail: yxuejin@ece.ucsb.edu).

Publisher Item Identifier 10.1109/LPT.2002.801057.

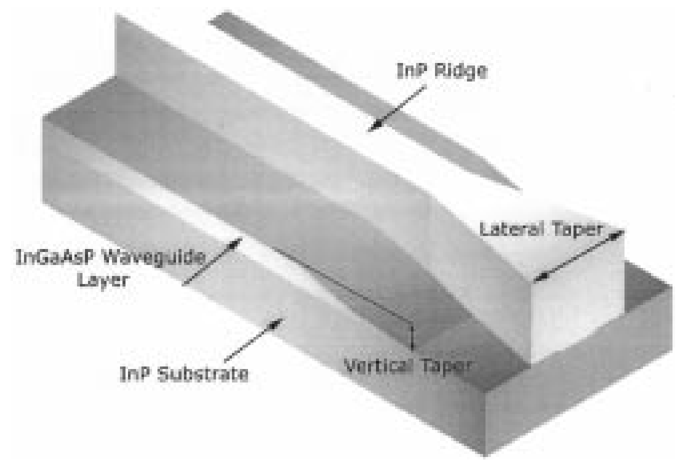


Fig. 1. Mode converter design schematic.

In this letter, we present a method to integrate mode converters with devices consisting of both active and passive waveguides, which is different from other methods reported [1]–[5]. It simplifies the process of device integration and reduces the number of regrowth steps to one. A new etchant used to make the vertical taper is safer to use than Bromine [6]. In order to demonstrate component integration using this process and to accurately measure the coupling efficiency, we fabricated an integrated sampled grating DRB laser with the mode-size converter (MC).

The mode converter is demonstrated to achieve fiber-to-InP waveguide coupling efficiencies of 70% using cleaved fiber and 86% with conical lensed fiber. Fiber alignment sensitivities are improved for cleaved fiber with measured tolerances of 3.7 and 3.0 $\mu$m along vertical and lateral directions, respectively.

## II. Vertical Taper Design and Device Processing

The mode converter structure is shown in Fig. 1. In order to prevent radiation losses at the taper, it is has been found that the local taper angle should be less than

$$\theta(z) \leq \frac{T(z)}{2\pi}\left(\beta_0(z) - \beta_r\right) \tag{1}$$

where $T(z)$ is the waveguide thickness, $\beta_0(z)$ is the local propagation constant, and $\beta_r$ is the propagation constant of the first radiation mode [7]. Using a nonlinear taper, this condition can be met while converting between different mode sizes in the shortest length possible [8], thereby minimizing the propagation loss. In order to produce the required taper profile, we designed our mask using a simple cubic formula given in [9]. Using three-dimensional (3-D) BPM modeling, it is possible to determine the optimum cleaving plane to achieve the best mode coupling into the fiber.

The integrated device uses an offset quantum well (QW) structure in order to combine active and passive waveguides onto a single planar circuit using a single regrowth. A multiple quantum well active region is grown on top of a 350-nm-thick low-bandgap (0.9 eV) quaternary waveguide. The two layers are separated by a 10-nm-thick InP stop-etch layer to enable the QWs to be removed from passive sections of the device using a selective wet etchant.

Fabrication of the device is accomplished by first creating the vertical tapers in the mode converter sections. Vertical tapers are made using bromine-based diffusion-limited wet etchant $HBr : HNO_3 : 15H_2O$. The tapers are created using an etch rate enhancement effect. The etch-rate enhancement depends on the ratio of mask and open area. Its maximum value is about 2.0 in this experiment. The etch rate measured is about 23 nm/min, which allows for very precise depth control during fabrication.

The next step is to selectively etch off the quantum wells only in the areas that will serve as passive sections of the device. Gratings are created in the mirror sections using holography/reactive ion etching; subsequently, a 2-$\mu$m-thick p-doped InP upper cladding layer with a $p^+$-InGaAs contact layer are regrown. It is important to emphasize that this is the only regrowth step required.

After regrowth, ridges in InP are formed using a combination of dry/wet chemical etching, followed by a proton implant to electrically isolate different electrodes. Finally, top and bottom metal contacts are evaporated using E-beam evaporation.

## III. Experimental Results

The SEM image of the fabricated taper is shown in Fig. 2. The surface profile was measured and is shown in Fig. 3. Its height was S-shaped and can be accurately modeled using a raised-sine curve [10]

$$H(x) = \frac{H}{L} \cdot x - \frac{H}{2\pi} \cdot \sin\left(\frac{2\pi \cdot x}{L}\right) \quad (2)$$

where $H$ is the total height of the taper, $L$ is the taper length, and $x$ is the distance measured from the output facet. This profile fulfilled the low radiation condition set by (1).

Near-field images with and without the mode converter at the laser output are shown in Fig. 4. The mode shape with mode converter was nearly circular. The full-width at half-maximum (FWHM) far-field divergence angles of the output intensity were measured to be $10.5^\circ \times 11.7^\circ$.

We have also measured the fiber coupling efficiencies for two cases: 1) a standard single-mode cleaved fiber and 2) a conical lensed fiber (Fig. 5). The efficiencies were measured relative to the total coupled power into a broad-area detector.

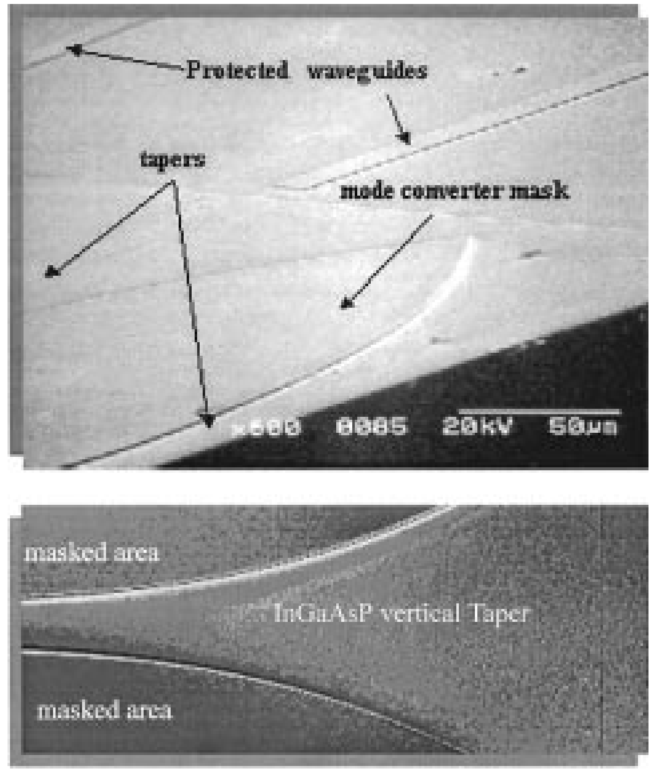


Fig. 2. SEM picture of fabricated tapers, with top view of a single taper.

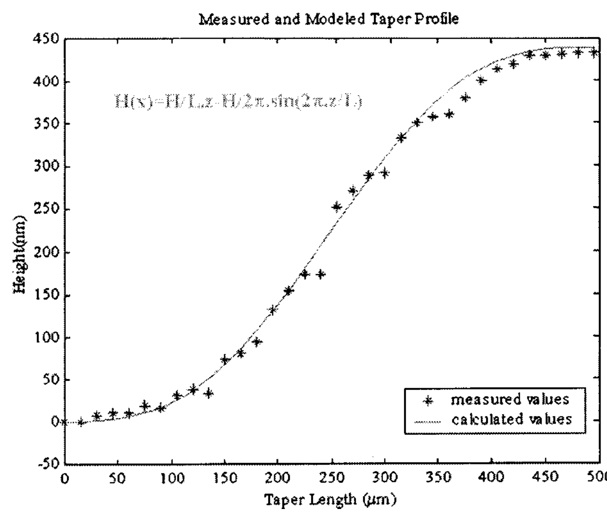


Fig. 3. Taper height versus distance—measurement and fitted results.

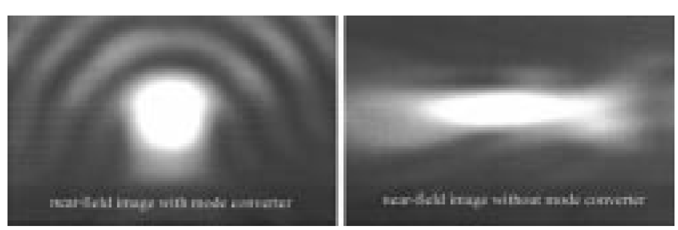

Fig. 4. Near-field images of the laser, with and without integrated mode converter.

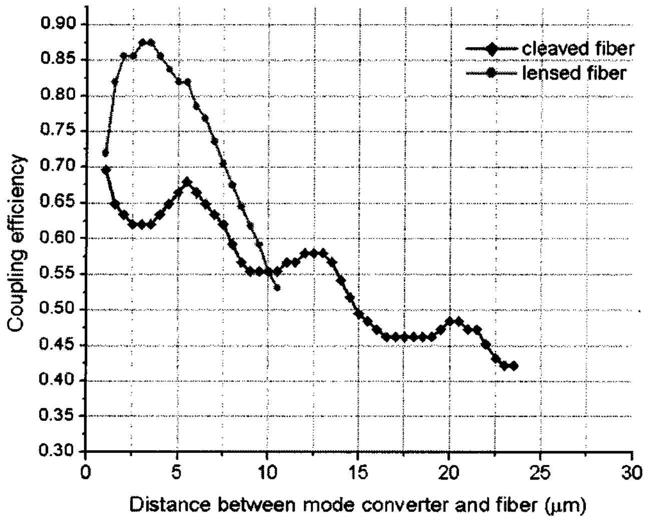


Fig. 5. Fiber coupling efficiencies measured for an integrated SGDBR laser with mode converter.

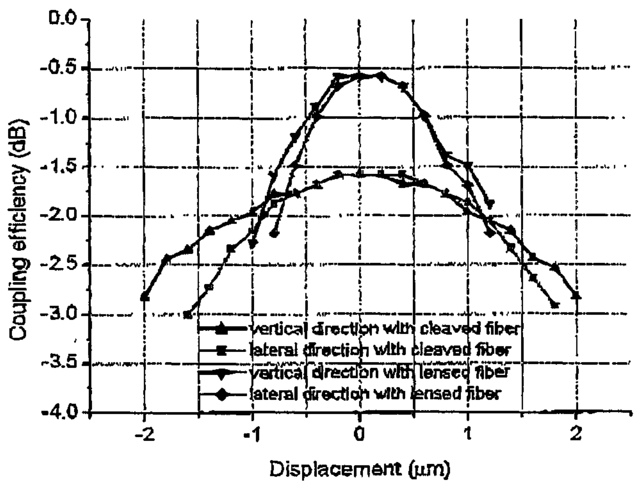


Fig. 6. Alignment tolerance measurements for different types of fibers.

A 70% coupling efficiency of fiber to SGDBR laser with mode converter has been achieved using a cleaved single-mode fiber with an 8.0-$\mu$m core and without AR coating. The maximum coupling efficiency using a conical lensed fiber without AR coating was over 86%. Fig. 5 also shows the dependence of coupling efficiency of cleaved and an uncoated conical lensed fiber to the laser/MC as a function of the distance between the fiber and the MC. Ripples in the coupling efficiency curves for the cleaved fiber were from reflections between the fiber and the facet.

Fig. 6 shows alignment tolerances for two types of fibers mentioned. For the cleaved fiber, 1-dB misalignment tolerances were $\pm 1.85$ and $\pm 1.5$ $\mu$m in the vertical and horizontal directions, respectively, as shown in Fig. 6. These alignment tolerances and coupling efficiencies make this device suitable for direct coupling with passive alignment to a silica waveguide on a planar lightwave circuit.

## IV. Conclusion

A new method for integration of optical mode converters with InP-based photonic integrated circuits is described and demonstrated. SGDBR laser monolithically integrated with a mode converter is reported. The fabrication process is simple with only two steps of epitaxial growth needed. The light spot size on the output facet of the chip was $4.0 \times 5$ $\mu m^2$ and its FWHM divergence angles of the output intensity in the far field were $10.5^\circ \times 11.7^\circ$. Due to a large mode size and small divergence angles in the far field, coupling efficiencies of 70% in a cleaved fiber and 86% in a conical-lensed fiber were measured. Large alignment tolerances ($\pm 1.85$ $\mu$m; $\pm 1.5$ $\mu$m) make direct coupling with passive alignment to a silica waveguide on a planar lightwave circuit possible. Therefore, monolithic integration of a mode-size converter with an InP-based photonic integrated circuit not only increases the coupled input–output power, but also has the potential to decrease the cost of device packaging with minimal alterations of the fabrication process.

## Acknowledgment

The authors would like to thank J. Getty of the ECE Department at the University of California at Santa Barbara for help with fabrication processes.

## References

[1] T. Brenner and H. Melchior, "Integrated optical modeshape adapters in InGaAsP/InP for efficient fiber-to-waveguide coupling," *IEEE Photon. Technol. Lett.*, vol. 5, pp. 1053–1056, 1993.

[2] G. A. Fish, B. Mason, L. A. Coldren, and S. P. DenBaars, "Compact, 1.55 $\mu$m spot-size converters for InP based photonic integrated circuits," in *Integrated Photonocs Research Conf.'99*, Santa Barbara, CA, July 19–21, paper RWD4, 375–377, pp. 141–143.

[3] U. Koren, R. B. Michael, B. I. Miller, M. G. Young, M. Chien, H. H. Yaffe, G. Raybon, and K. Dreyer, "EA modulator with passive waveguide spotsize converters," *Electron. Lett.*, vol. 30, pp. 1852–1853, 1994.

[4] C.-H. Chen, S. C. Shunk, U. Koren, M. Chien, B. I. Miller, K. F. Dreyer, H. M. Presby, and R. G. Ahrens, "Semiconductor optical amplifier array coupled to uncoated flat-end fibers with integrated beam expanders and $TiO_2$ antireflection coatings," *IEEE J. Select. Topics Quant. Electron.*, vol. 3, pp. 1421–1428, June 1997.

[5] H. Jeon, J.-M. Verdiell, M. Ziari, and A. Mathur, "High-power low-divergence semiconductor lasers for GaAs-based 980-nm and InP-based 1550nm applications," *IEEE J. Select. Topics Quantum Electron.*, vol. 30, pp. 1344–1350, June 1997.

[6] X. Yan, M. Mašanović, and D. Blumenthal, "A new simple process for optical mode converter integrated with active and passive waveguides in InGaAsP/InP," in *Integrated Photonocs Res. Conf. 2001*, Monterey, CA, June 11–13, 2001, paper IMG4.

[7] J. D. Love, "Application of a low-loss criterion to optical waveguides and devices," *Proc. Inst. Elect. Eng.*, vol. 136, no. 4, pp. 225–228, 1989.

[8] G. Fish, "InGaAsP/InP based photonic integrated circuits for optical switching," Ph.D. dissertation, ECE Dept. Tech. Rep., UCSB, 1999.

[9] K. Kawano, M. Kohtoku, H. Okamoto, Y. Itaya, and M. Naganuma, "Coupling and conversion characteristics of spot-size-converter integrated laser diodes," *IEEE J. Select. Topics Quant. Electron.*, vol. 3, pp. 1351–1360, June 1997.

[10] W. J. Minford, S. K. Korotky, and R. C. Alferness, "Low-loss Ti : $LiNbO_3$ waveguide bends at $\lambda = 1.3$ $\mu$m," *IEEE J. Quantum Electron.*, vol. QE-18, pp. 1802–1813, Oct. 1982.